ENGINEERING RESEARCH JOURNAL (ERJ)
Vol. 51, No. 4 October. 2022, pp.30-41
Journal Homepage: erj.bu.edu.eg

Numerical Investigation for Ejectors Performance with Different Geometrical Parameters

Dina Khaled[a*], Ibrahim M. Shahin[a], Ahmed A. Abdulatif[a] and ShehataM.H.[a]
[a] Mechanical Engineering, Faculty of Engineering (Shoubra), Benha University, Cairo, Egypt
* Corresponding author

Abstract: The present study used computational fluid dynamics (CFD) technique to examine the impactsof the nozzle exit position (NXP), the area ratio of the constant area zone to the primary nozzle throat, and the mixing chamber diameter (D_m) on the ratio of entrainment and also the performance of the ejector. The effect of the parameters is explained by using different geometric structures under the same boundary conditions. The simulation validated by using the disseminationof static pressure and the given experimental data of entrainment ratio (ER)which is available in the literature. It is found that, the simulation error between the experimental data and the (CFD) results of entrainment ratio of the ejector are 10.4% and 1.5% for pressures of 143.3 kPa and 270 kPa, respectively. The results show that the steam ejector performance is sensitively affected by increasing the entrainment ratio.

KEYWORDS:: Ejector; Entrainment ratio; area ratio; NXP; mixing chamber diameter.

1. INTRODUCTION

Ejectors offer a simple method to produce vacuum. Ejectors are based on the venture vital and work by passing thought process steam or gas through a growing spout rather than moving parts to compress gas. The steam converts potential energy to kinetic energy as it converts pressure into which makes a vacuum within the blending chamber zone to draw in vapors or gases. The motive fluid and suction gas are totally blended and then passed through the diffuser, where the gases velocity is changed over into sufficient pressure to meet the foreordained outlet pressure. There are many advantages of ejectors over other types of vacuum producing devices such as the simplicity of the design as its compact and reliable. Due to the comparison between ejector's pumps with the other types of devices, they are low in their cost. The maintenance of ejectors is easy as there are no moving parts to wear or break and easy to install due to light in weight, and don't require foundations.

Nomenclature

Symbols	Description
E	Total energy, J
K	Turbulent kinetic energy, J/kg
W	Entrainment ratio
P	Pressure, Pa
T	Static temperature, C
t	Turbulent kinetic energy, J/kg
U	Velocity, m/s

x	Streamwise distance, m
y	Spanwise distance, m
μ	Energetic viscosity, N s/m2
μ_t	Viscosity of turbulent, N s/m2
α	Tuning parameter
ρ	Density of the mixture, kg/m3
τij	Stress tensor
ω	Dissipation rate, 1/s
U	The component of velocity
$\mathcal{X}$	The Cartesian direction
μ_{eff}	The effective molecular dynamic viscosity
Fs	Factor of safety
r	Grid refinement ratio
GCI	Grid Convergence Index
i,j	Cartesian Tensor Notation
NXP	Nozzle Exit Position

Ejectors are being used widely in many applications world-wide including Refinery vacuum systems, Thermal compressor, Crystallization, Vacuum distillation units, Crude oil distillation, and Evaporative cool.

It mainly consists of fundamental four sections, the section of primary nozzle, the section of mixing chamber, the section of constant area, and the diffuser. The primary nozzle converts the high pressure and low velocity into high velocity at a low static pressure. The velocity of the fluid inside the nozzle increases to reach sonic velocity at the nozzle throat section, then the velocity increases till the nozzle exit with a very low pressure Al Doori et al. [1]. Figure 1 shows the schematic view of an idealized process in an ejector.

The low pressure at the end of the primary nozzle at a supersonic speed is the main reason of entering the secondary fluid to the mixing chamber section, then the two streams of primary and secondary are mixing and raise the rapid pressure in the section of constant area, and the stream is decelerated to a subsonic speed in the diffuser due to the created shock waves.

The curve of performance of an ejector is separated by the critical back pressure and the break-down back pressure into three zones choked flow zone, un-choked flow zone and reversed flow zone as shown in Figure 2.

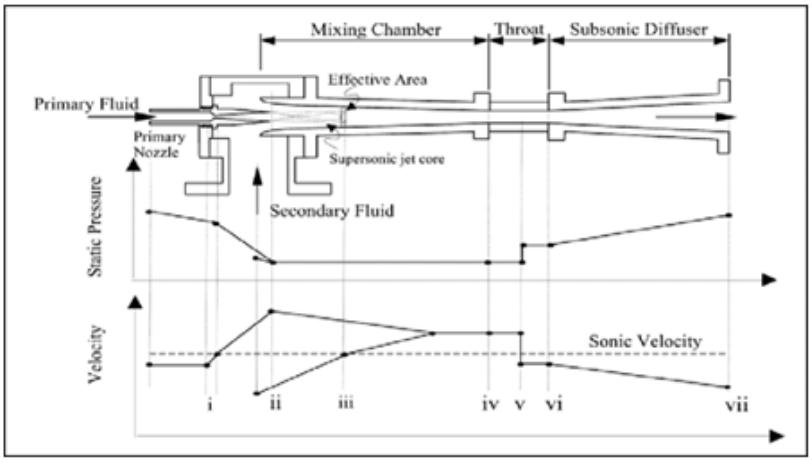

FIG 1. Schematic view and the variety of stream pressure and velocity as a work of area along an ejector from Sriveerakul, T. et al. [2]

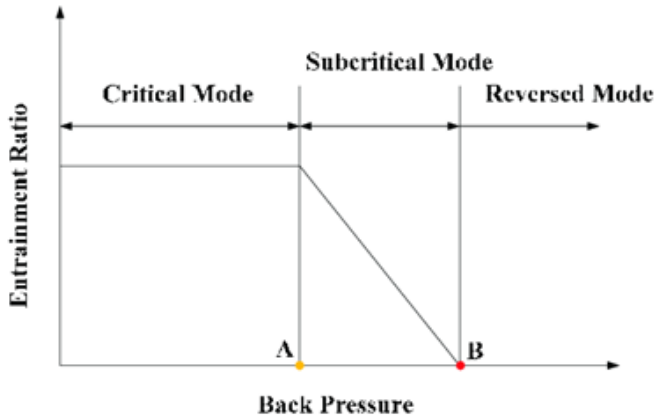

FIG 2. Ejector performance characteristics.

Many studies focused on the impact of changing different parameters on the performance of an ejector. Sriveerakul et al. [2] reported that CFD technology was a pioneer study in foreseeing execution of a steam ejector utilized in refrigeration applications. A steam jet refrigeration is one of the most suitable systems for environment situations. The CFD was an important tool in foreseeing ejector execution. Moreover, gives a more way better understanding within flow and blending processes inside the ejector. Navid Sharifi et al.[3] displayed the explanatory displaying of the impacts of damp steam on the streamlined features and thermodynamics execution of steam ejectors. Also, focused on the thermodynamics parameters of ejectors relationship in the wet. It has shown that steam nucleation could be a predominant wonder in supersonic steam flows. Tang, Yongzhi et al.[4] presented how to optimize the parameters of the assistant entrance with its opening position, width and the angle of inclination to create full utilize of the potential of pressure within the ejector throat to improve the performance. It has been analyzed numerically, and obtained the assistant influence of entraining entrance parameters on stream areas and mass flow rate. Ghorbanzadeh et al.[5] presented numerically investigation of the parameters influence on the ejector performance by tackling the unfaltering the convergent-divergent (C-D) spout position for each working condition and to bring out the influence of reflected stun waves and boundary layer within the consistent zone blending chamber on the execution of the ejector. The development of Computational Fluid Dynamics or CFD technology has been an effective tool and widely used in the study of ejectors. On the other hand, CFD method is a useful approach to investigate the flow behavior and blending processes in ejectors Tang, Yongzhi et al.[6]. The CFD tool has been connected in different works to study the effect of operating parameters and geometrical on the performance of ejectors Yang et al. [7]. Yadav et al. [8] studied the impact of working pressures on the stun waves and jet behavior in ejector. MK Ji et al. [9] presented a CFD model on the blending process in an ejector to estimate the effect of using different structures on the entrainment ratio. Many of examinations have centered on the parameters that impact the execution of ejector counting the working conditions, the geometry of the ejector and the spout exit position inside the blending chamber by examining the impact of joining point and the blending chamber distance acrossS. Aphornratana et al. [10], and Ariafar et al. [11].

In this numerical study, CFD has been investigated the influence of blending between the primary stream and the secondary streamon the ejector ratio of the entrainment. The ejector is simulated and its execution compared and surveyed with exploratory information beneath rearranged conditions. There are two approaches to approval are received. The ejector is recreated and compared its execution with test information beneath the same boundary conditions.Dong et al. [12] presented a numerical study of the mixing chamber

length influence on the steam ejector and it's observed that the entrainment ration increases then decreases with increasing the length of the mixing chamber.Zhang et al. [13] studied and presented a modified condensation model in order to investigate the internal flow structure of steam ejector. Furthermore, to optimize the primary nozzle of the ejector. The accuracy of this model has been tested in a supersonic nozzle and a steam ejector to determine the model feasibility. Different models had been compared to prove the advantage of modified model and the model is used to estimate the optimization program

2.COMPUTATIONAL MODEL

2. 2.1. Governing equations

Continuity, momentum, and energy equations are used in the computational fluid dynamics based on the suspicions can be composed as takes after:

The equation of continuity:

$$\frac{\partial \rho}{\partial t} + \frac{\partial}{\partial x_t}(\rho U_i) = 0 \quad (1)$$

Where:

ρ is density, U_i is the component of velocity along $\mathcal{X}_i$ which is the Cartesian direction, and time t.

The equation of momentum:

$$\frac{\partial}{\partial t}(\rho U_i) + \frac{\partial}{\partial xi}\left(\rho U_i U_j\right) = -\frac{\partial p}{\partial x_i} + \frac{\partial \tau_{ij}}{\partial x_j} \quad (2)$$

Where:

P and τ are the pressure and the shear stress sensor.

The equation of energy:

$$\frac{\partial}{\partial t}(\rho E) + \frac{\partial}{\partial xi}(U_i(\rho E + P) = \vec{\nabla}.(\propto_{eff} \frac{\partial T}{\partial x_i} + U_j(\tau_{ij})) \quad (3)$$

With

$$\tau_{ij} = \mu_{eff}\left(\frac{\partial U_i}{\partial x_j} + \frac{\partial U_j}{\partial x_i}\right) - \frac{2}{3}\mu_{eff}\frac{\partial U_k}{\partial x_k}\delta_{ij} \quad (4)$$

Where:

E is the total energy and$\mu_{eff}$is the effective molecular dynamic viscosity.

2.2. The Model of Turbulence

It is exceptionally vital and fundamental to select the most excellent turbulence show for examine and foresee the ejector execution. While the blending of two streams and the speeds into the ejector are disseminated non-uniformly, so the stream cannot be recreated by streamlined in viscid or thick in viscid plans. This non-uniformly vortices create turbulence to the stream, and this created vitality misfortune when the essential and auxiliary streams are blended. In addition, there will be additional vitality misfortune produced whereas the contact between the essential stream and the essential spout, and between the auxiliary stream and the divider of the ejector, moreover between the blending streams and the blending tube divider which can influence the stream characteristics inside the ejector.

In this work, the SST k−ω model has been used to provide a better prediction of flow separation and also too it has the capacity to account for the transport of the foremost shear stretch in unfavorable weight point boundary layers. It is the foremost preeminent commonly utilized illustrate inside the industry given its tall precision to cost proportion. According to Besagni et al.[14], the k-ω SST model yielded the most excellent comes about for the numerical confirmation of worldwide and neighborhood stream parameters gotten from the exploratory comes about. The communicated expressed that for future numerical thinks about concerned with the ejector, utilize of the SST k-ω demonstrate was proposed.

The governing equations for this model are as follows:

$$\frac{\partial(\rho K)}{\partial t} + \frac{\partial}{\partial x_i}(\rho k U_i) = \frac{\partial}{\partial x_j}\left[\left(\mu + \frac{\mu_t}{\sigma_k}\right)\frac{\partial k}{\partial x_j}\right] + G_k - Y_k + S_k \quad (5)$$

$$\frac{\partial(\rho\omega)}{\partial t} + \frac{\partial}{\partial x_i}(\rho\omega U_i) = \frac{\partial}{\partial x_j}\left[\left(\mu + \frac{\mu_t}{\sigma_\omega}\right)\frac{\partial \omega}{\partial x_j}\right] + G_\omega - Y_\omega + D_\omega + S_\omega \quad (6)$$

Where:

k is the turbulent kinetic energy and ω is the specific dissipation rate.

2.3. Numerical Modeling

Computational Fluid Dynamics (CFD) used to monitor and study the fluid stream behavior within ejector. It employs the finite volume way for discretization. The non-linear equations in the steady state condition was solved by an implicit density based solver with second order upwind spatial discretization.

In this work, commercial software (ICEM 2019 R2) is used to generate 2D grid. The schematic view of the particular ejector was displayed in Figure 3. The ejector model consists of main different zones as the following; (i) suction zone where primary flow and secondary flow enter, (ii) Mixing chamber zone, (iii) Constant area zone, and (iv) Subsonic diffuser.

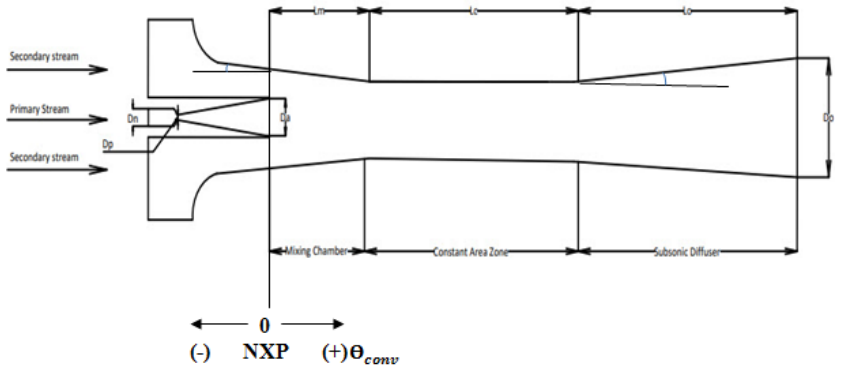

FIG 3. Schematic representation of the zones for a typical ejector.

2.4. Geometry and operating conditions of the Ejector

The Ejector dimensions, which was outlined and worked in a refrigeration framework Al Doori et al. [1], are given in Table 1.

Table 1Dimension of the ejector:

Geometrical parameters	Size (mm)
The inlet diameter of Primary nozzle (D_n)	10
The throat diameter of Primary nozzle(D_p)	3.2
The outlet diameter of Primary nozzle(D_a)	13.6
The divergent length of Primary nozzle	59.5
The inlet diameter of Mixing chamber	37
The length of Mixing chamber(L_m)	155
The diameter of Constant area zone	25.4
The length of Constant area zone(L_c)	75
The length of diffuser(L_o)	210
The outlet diameter of diffuser(D_o)	50
Pre- Mixing Chamber converging angle Θ_{conv}	10.3º
Subsonic diffuser divergence angle Θ_d	24.2º

The exit position of primary nozzle, which is described as the space between the primary nozzle exit and the mixing chamber entrance was at +6 mm. Figure 4 shows the view of the mesh structure and Figure 5 shows the details of the structure. The grid was generated according to the structured quadrilateral elements. The structure grid consists of 98,460.00 elements in order to grid independent solutions.

FIG 4. View of the mesh structure of the ejector.

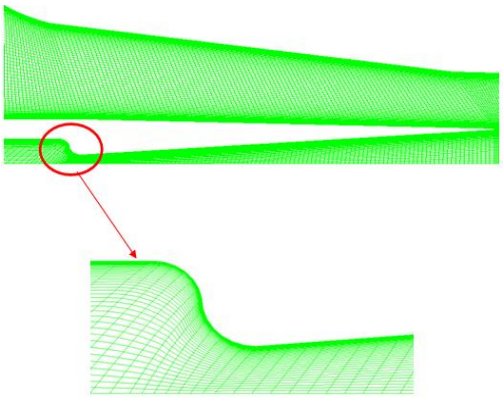

FIG 5. Detailed view of the mesh structure of the ejector

In this study, steam was used as a fluid of the model with the assumptions of an ideal gas. The properties of the working fluid as given in FLUENT database are shown in Table 2.

Table 2 Fluid properties

Properties	Value
Density	Ideal gas model
Conductivity	0.0261 W/mK
Viscosity	1.34E-05
Molecular weight	18.015 kg/kgmol

The inlet operating conditions for the primary stream and secondary stream were set and indicated the type of inlet pressure. On the other hand, the ejector outlet operating conditions was set to the type of outlet pressure. All wall surfaces of the ejector were set as the adiabatic walls. The summary of the inlet operating conditions and outlet operating conditions were given in Table 3.

Table 3 Ejector operating conditions:

Stream	Pressure (kpa)	Temperature (K)
Primary stream	270	403
Secondary stream	1.2	283
Discharge	6	-

3. VALIDATION WITH EXPERIMENTAL RESULTS

3.1. Validation of static pressure

The main purpose of this study is to focus and center on the effect of blending the primary fluid flow with the secondary fluid flow on the ejector ratio of entrainment. Validation of the numerical method is represented for the distribution ofpressure-static along the wall of ejector reproached with the data of experimental for different pressures 270 kpa and 1.2 kpa for the primary flow and secondary flow, plus 6 kpa for the outlet pressure as shown in Figure 6.

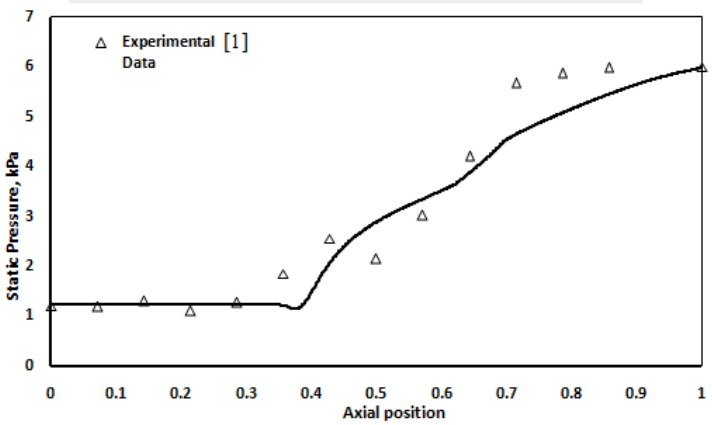

FIG 6. Static pressure distribution along the ejector wall.

It is observed that the pressure profile of our model is matched with the pressure profile of the experiment under the ideal gas assumptions. Figure 7 shows the distribution of Mach number.

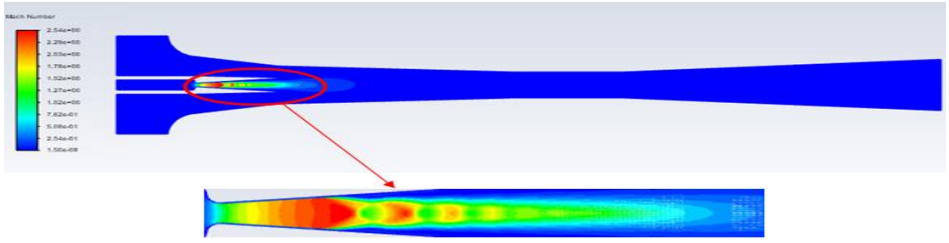

FIG 7. The distribution of Mach number.
Pp= 270 kPa, Mixing Chamber Diameter= 37 mm

3.2. Validation of entrainment ratio

In this section, the entrainment ratio of the steam ejector values which obtained with the experimental data reported in Al-Doori et al. [1] and the CFD simulations as presented in Table 4. Reenactments were executed for values of essential weights of 143.3, 270 amd 476 kpa, in any case auxiliary and outlet weights remained steady at 1.6 kpa and 4.2 kpa, individually

$$w = \frac{Secondary fluid mass flow rate}{Primary fluid mass flow rate}$$

Table 4 Experimental data Al-Dooriet al. [1] and CFD simulation results for the entrainment ratio.

The pressure of primary fluid (kpa)	The pressure of secondary fluid (kpa)	Pressure-outlet (kpa)	Experimental ratio of entrainment	Simulation ratio of entrainment	Simulation error (%)
143.3	1.6	4.2	0.44	0.485	10.2
270			0.33	0.335	7.5
476				0.214	

It is observed that the ejector ratio of entrainment decreases with increasing the stream of primary pressure. The ratio of entrainment decreases from 0.485 to a value of 0.214 at the primary stream pressures 143.3 kPa and 476 kPa, respectively. The simulation error between the experimental data and the CFD results for the ratio of entrainment of the ejector are given in table 4. Figure 8 shows Mach number distribution for the three different pressure.

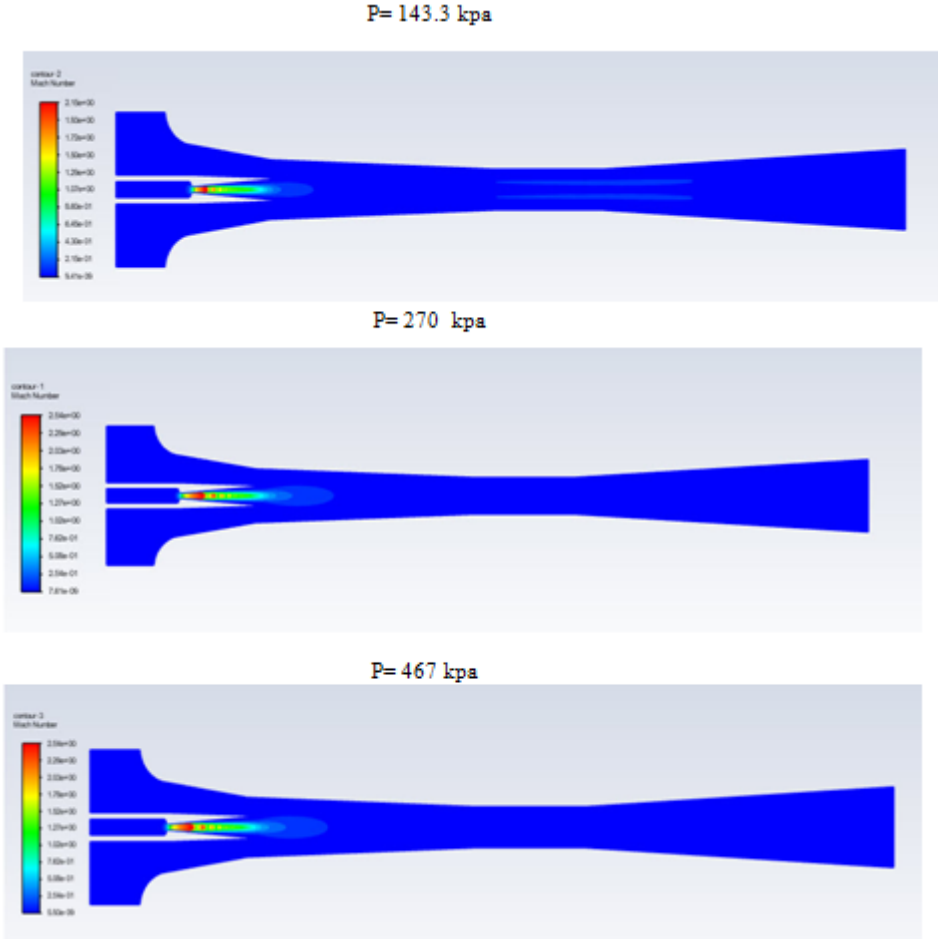

FIG 8. Mach number distribution for three different pressures

.

3.3. Grid Independence Study

The grid independence study is a formal approach to obtaining grid independency of the CFD solution using Grid Convergence Index (GCI). There are many advantages of (GCI) as it is used to give an objective measure of uncertainty. The study of independence grid is carried to decide this ideal point where a decently precise arrangement for the issue is found at the cost of slightest computational assets. When utilizing an ideal work, the precision of the comes about are great sufficient to capture the vital stream highlights. A coarse lattice will not capture all the stream highlights, and a better work will donate an

arrangement of a small higher precision than required but at the cost of computational control and time. This is often the reason for performing a work freedom consider. By beginning with a coarse mesh and unravel, it's watched that there's a difference in comes about as the work got better. But, there's a limit. When it's observed that there's no any changes in the results even after the mesh became finer. Then it is observed that the grid independence has been achieved. At this point, the mesh will be fine sufficient to capture the foremost complex points of interest of the flow, which is why making it finer will not make any changes in the results.

Grid Convergence Index Method:

$$GCI_{fine} = F_s\left(\frac{f_2 - f_1}{f_1}\right)\left(\frac{1}{r^p - 1}\right) \quad (7)$$

$$GCI_{coarse} = F_s\left(\frac{f_2 - f_1}{f_1}\right)\left(\frac{r^p}{r^p - 1}\right) \quad (8)$$

Where:

Fs is factor of safety and r is grid refinement ratio.

In arrange to decide the number of components constituted the computational space and to watch the precision and unwavering quality of numerical work, a rudimentary work freedom think about was conducted. Five work structures were made. In Table 5 the comes about for each work structure arrangement are given and were compared with each other, and Figure 9 shows the difference between the mesh of five different mesh structure.

Table 5 The results of each mesh structure solution.

Case No.	Cell No.	ER
1	47700	1.05
2	64540	0.77
3	98460	0.335
4	159660	0.281
5	220860	0.279

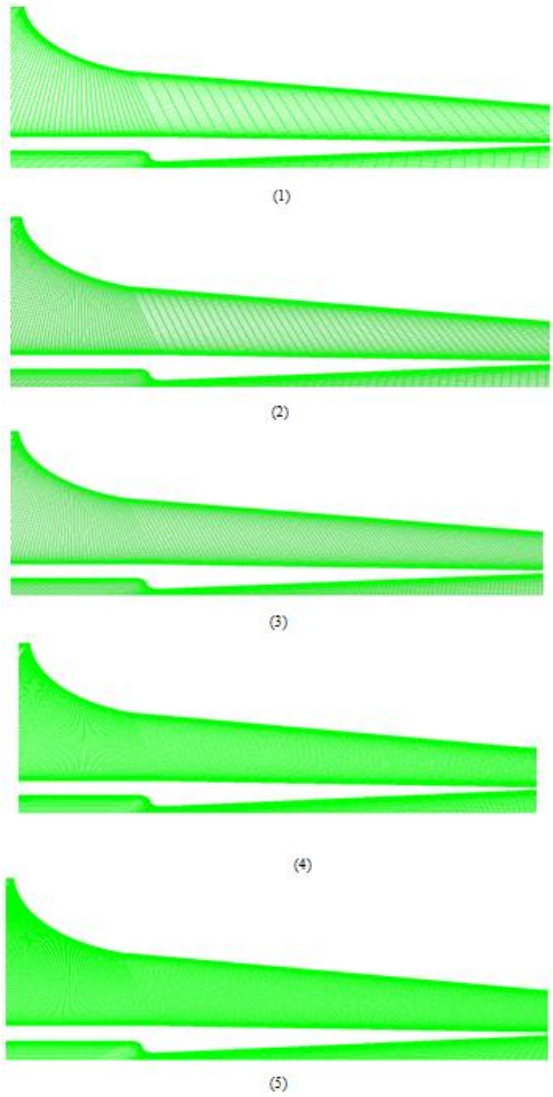

FIG 9. Detailed view of five mesh structures

4. RESULTS AND DISCUSSION

The design of the ejector has an impact on the performance of the system, and there are two standards to evaluate the ejector performance, one is critical back pressure and the most common one is the entrainment ratio and it's known as the factor that decides the performance of an ejector. The entrainment ratio is affected by geometry and operating conditions. The results were performed for different primary pressures (143.3, 270, 476) kPa. The secondary pressure and the outlet pressure remained as they are(1.6, 4.2)kPa. The focus was on three important parameters, the exit nozzle position (NXP), the mixing chamber diameter, and the constant area zone diameter, and studied the results of five different ranges for each parameter. The

pressure and temperature values for different operating conditions are given in Table 6.

Table 6 Ejector temperature and pressure:

Flow	Temperature (K)	Pressure (kpa)
Primary	383, 403, 423	143.3, 270, 476
Secondary	287	1.6
Discharge	-	4.2

The outlet position of primary nozzle exit position is the distance between the plane of the outlet of primary nozzle and the plane of inlet of the mixing chamber. NXP has strong influence on ejectors performance. Moreover, NXP plays an important role in the ejector performance as the location of the outlet position of the primary nozzle influenced the ratio of entrainment and the critical back pressure. This study used different ranges of NXP (-6, -3, 0, 3, 6) mm under the same operating conditions. It's observed that he increasing speed of the auxiliary stream by the essential stream within the steady pressure blending zone takes a longer time when the nozzle is moved away the mixing zone, so to maximize the ejector performance, it's suggested to use an ejector with movable primary nozzle. Also, it's observed that the optimum NXP depended on the operating conditions, as it cannot meet all working operating conditions.

Figure 10 shows the result for the entrainment ratio with different nozzle exit positions (NXP) at different primary pressures 143.3, 270, and 476 kpa respectively. The entrainment ratio changed over the different ranges of NXP over different pressures. At 143.3 kpa the entrainment ratio was 3.23 at -6 mm, 3.46 at -3 mm, 3.95 at 0 mm, 3.86 at 3 mm, and 3.01 at 6 mm. At 270 kpa the entrainment ratio was 2.86 at -6 mm, 2.98 at -3 mm, 3.7 at 0 mm, 3.21 at 3 mm, and 2.42 at 6 mm. At 476 kpa the entrainment ratio was 2.01 at -6 mm, 2.66 at -3 mm, 3.13 at 0 mm, 3.01 at 3 mm, and 2.3 at 6 mm the ejector for each case of the NXP ranges at each used primary pressures.

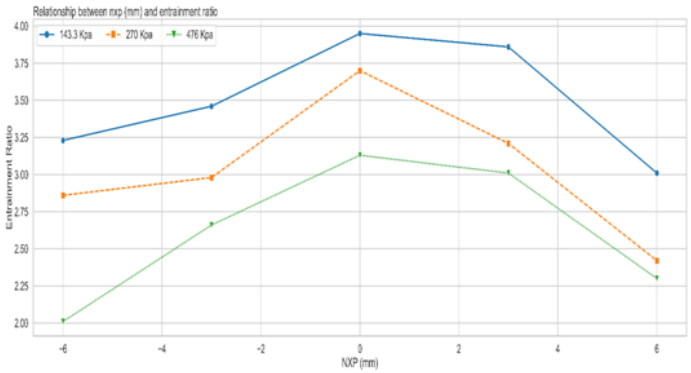

FIG 10. Result for the entrainment ratio with different nozzle exit positions (NXP) at different primary pressures.

The mixing chamber is the convergent duct-constant section, and its structure is one of the most important parameters which has a great effect on the ejector performance. This study used variable values of mixing chamber diameter (35, 36, 37, 38, and 39) mm under the same operating conditions.

It's observed that to decrease the energy loss through the diffuser, the mixing fluid has to be more uniform, so the outlet pressure will be high, and this is very important for ejector to use low grade energy as power. It's observed that the entrainment ratio is reducing by decreasing the mixing chamber diameter. Figure 11 shows the result for the entrainment ratio with different mixing chamber diameter ranges at different primary pressures 143.3, 270, and 476 kpa respectively.

The entrainment ratio changed over the different ranges of mixing chamber diameters over different primary pressures.

At 143.3 kpa the entrainment ratio was 1.92 at 35 mm, 2.32 at 36 mm, 2.56 at 37 mm, 3.32 at 38 mm, and 3.69 at 39 mm. At 270 kpa the entrainment ratio was 1.65 at 35 mm, 1.79 at 36 mm, 2.23 at 37 mm, 2.64 at 38 mm, and

3.50 at 39 mm. At 476 kpa the entrainment ratio was 0.99 at 35 mm, 1.38 at 36 mm, 1.54 at 37 mm, 2.45 at 38 mm, and 3.10 at 39 mm.

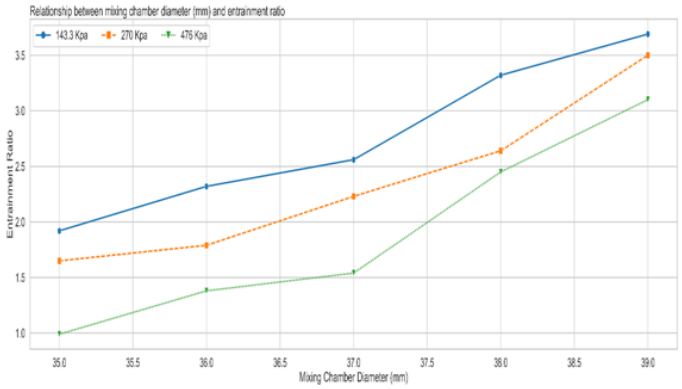

FIG 11. Result for the entrainment ratio with different mixing chamber diameters at different primary pressures.

The area ratio of the ejector is the relation between the zone of the constant area to the zone of the throat of primary nozzle. Depending on the operating conditions of the ejector, an optimal area ratio is exited and it's increased with the temperature of the generator, decreased with the temperature of the condenser, and it's less affected with the variation in the temperature of the evaporator. Moreover, the effect of the area ratio is well established more than NXP. This study used variable values of constant area diameter (23.4, 24.4, 25.4, 26.4, and 27.4) mm, while the diameter of the primary nozzle throat remained constant under the same operating conditions. It's observed that the secondary flow doesn't reach the conditions of sonic according to the primary nozzle litter energy beyond the optimum area ratio, and the decrease in the performance of ejector can be clarified with over expansion of the primary nozzle due to the high mass flow rate. Furthermore, the decreasing of area ratio, decreases the efficiency and the performance of the ejector. Figure 12 shows the result for the entrainment ratio with different mixing chamber diameter ranges at different primary pressures 143.3, 270, and 476 kpa respectively. The entrainment ratio changed over the different ranges of area ratio over different primary pressures. At 143.3 kpa the entrainment ratio was 1.09 at 53.5 mm, 1.23 at 58.1 mm, 1.62 at 63 mm, 1.85 at 68 mm, and 2.1 at 73.3 mm. At 270 kpa the entrainment ratio was 0.85 at 53.5 mm, 0.9 at 58.1 mm, 1.25 at 63 mm, 1.45 at 68 mm, and 1.89 at 73.3 mm. At 476 kpa the entrainment ratio was 0.65 at 53.5 mm, 0.78 at 58.1 mm, 0.82 at 63 mm, 1.10 at 68 mm, and 1.57 at 73.3 mm.

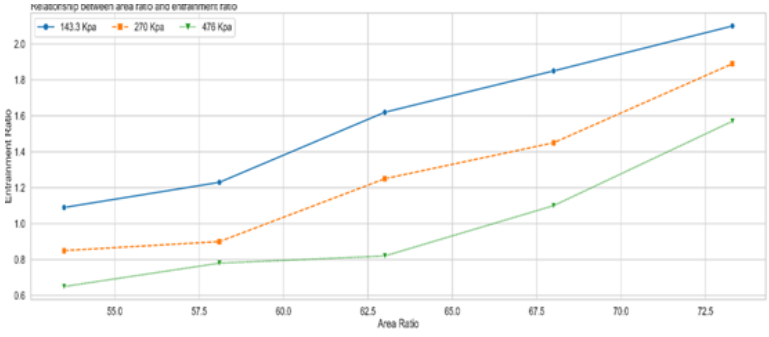

FIG 12. Result for the entrainment ratio with different area ratios at different primarypressures

5. CONCLUSION

This work investigated the effect of the blending between primary stream and secondary stream on the ratio of entrainment of the ejector, and discussed the effect of different parameters such as the exit nozzle position (NXP), the mixing chamber diameter, and the constant area zone diameter on the ejector performance under different boundary conditions and how can it be improved. The results can be summarized based on studies as follows:

- The increasing speed of the auxiliary stream by the essential stream within the consistent pressure blending zone takes a longer time when the spout is moved absent the blending zone, so to maximize the ejector performance, it's suggested to use an ejector with movable primary nozzle
- The location of NXP is influenced the condemnatory back pressure and the ratio of entrainment
- The optimum NXP depended on the operating conditions, as it cannot meet all working operating conditions
- NXP plays a necessary role in the ejector performance
- When operating in critical mode with a shock diffuser, the constant area diameter improved the ejector performance
- The efficiency decreases with decreasing the ejector area ratio
- Based on the operating conditions of the ejector, an optimal area ratio is exited and it's increased with the temperature of the generator, decreased with the temperature of the condenser, and it's less affected with the variation in the temperature of the evaporator
- The decreasing of area ratio, decreases the efficiency and the performance of the ejector
- The secondary flow doesn't reach the conditions of sonic according to the primary nozzle litter energy beyond the optimum area ratio, and the decrease in the performance of ejector can be clarified by over expansion of the primary nozzle due to the high mass flow rate
- The effect of the area ratio is well established more than NXP
- Decreasing the mixing chamber diameter leads to decrease the secondary flow rate as the entrance space of it into mixing channel is limited

REFERENCES

[1] Al-Doori GFL. Investigation of refrigeration system steam ejector performance through experiments and computational simulations. University of Southern Queensland; 2013.

[2] Sriveerakul, Thanarath, Satha Aphornratana, and KanjanaponChunnanond. "Performance prediction of steam ejector using computational fluid dynamics: Part 1. Validation of the CFD results." International Journal of Thermal Sciences 46, no. 8 (2007): 812-822.

[3] Sharifi, Navid, MasoudBoroomand, and Majid Sharifi. "Numerical assessment of steam nucleation on thermodynamic performance of steam ejectors." Applied Thermal Engineering 52, no. 2 (2013): 449-459.

[4] Tang, Yongzhi, Zhongliang Liu, Yanxia Li, Can Shi, and Hongqiang Wu. "Performance improvement of steam ejectors under designed parameters with auxiliary entrainment and structure optimization for high energy efficiency." Energy Conversion and Management 153 (2017): 12-21.

[5] Ghorbanzadeh, Sepehr, and EsmailLakzian. "Enhancement of the air ejector performance: primary nozzle and mixing chamber investigation." Journal of the Brazilian Society of Mechanical Sciences and Engineering 40, no. 2 (2018): 45.

[6] Tang, Yongzhi, Yanxia Li, Zhongliang Liu, Hongqiang Wu, and Weina Fu. "A novel steam ejector with auxiliary entrainment for energy conservation and performance optimization." Energy Conversion and Management 148 (2017): 210-221.

[7] Yang K, Lee H, Jung H. Numerical prediction of jet behavior of thermal vapor compressor. Desalin Water Treat 2011;33(1e3):248e54.

[8] Yadav RL, Patwardhan AW. Design aspects of ejectors: effects of suction chamber geometry. ChemEngSci 2008;63(15):3886e97.

[9] Ji M, Utomo T, Woo J, Lee Y, Jeong H, Chung H. CFD investigation on the flow structure inside thermo vapor compressor. Energy 2010;35(6):2694e702.

[10] Chunnanond K, Aphornratana S. An experimental investigation of a steam ejector refrigerator: the analysis of the pressure profile along the ejector. ApplThermEng 2004;24(2):311e22.

[11] Ariafar, Kavous, David Buttsworth, Ghassan Al-Doori, and Navid Sharifi. "Mixing layer effects on the entrainment ratio in steam ejectors through ideal gas computational simulations." Energy 95 (2016): 380-392.

[12] Dong, Jingming, Qiuyu Hu, Mengqi Yu, Zhitao Han, Wenbin Cui, Daliong Liang, Hongbin Ma, and Xinxiang Pan. "Numerical investigation on the influence of mixing chamber length on steam ejector performance." *Applied Thermal Engineering* 174 (2020): 115204.

[13] Zhang, Guojie, SławomirDykas, Sichong Yang, Xinzhe Zhang, Hang Li, and Junlei Wang. "Optimization of the primary nozzle based on a modified condensation model in a steam ejector." *Applied Thermal Engineering* 171 (2020): 115090.

[14] Besagni, Giorgio, and Fabio Inzoli. "The effect of liquid phase properties on bubble column fluid dynamics: Gas holdup, flow regime transition, bubble size distributions and shapes, interfacial areas and foaming phenomena." Chemical Engineering Science 170 (2017): 270-296.